Chapter 7
Polymer- and Carbon-Based Nanofibres for Energy Storage

Alexandra Ho, Suxi Wang, Xu Li and Haifei Zhang

Abstract There is ever-increasing demand for energy worldwide. The constant use of energy particularly in portable devices and vehicles has required highly efficient and high-capacity energy storage. Materials research is at the front of addressing the society's demand for energy storage. This chapter focuses on the fabrication and use of polymer and carbon-based nanofibers for energy storage. The widely used fabrication methods such as chemical vapour deposition, electrospinning and the recently developed methods including controlled freezing and gelation for nanofibers have been described. Upon the preparation of polymer nanofibers, carbon nanofibers can be produced by pyrolysis under inert atmosphere. We then review the applications of carbon-based nanofibers in different types of rechargeable batteries and supercapacitors. The chapter is completed with conclusion and outlook.

7.1 Introduction

With the increase in demand for energy, there must be a corresponding increase in energy production which in turn leads to issues in supply and demand. Renewable energy sources such as wind and solar light demonstrate a great potential for reducing the dependence on fossil fuels and thus the production of greenhouse gas emissions [1]. Energy requirements are variable throughout the day, and a balance must be achieved that avoids undersupply, but also prevents wasting through overproduction. As the world looks towards renewable energy sources, we need a reliable electricity

A. Ho · H. Zhang (✉)
Department of Chemistry, University of Liverpool, Oxford Street, Liverpool L69 7ZD, UK
e-mail: zhanghf@liverpool.ac.uk

A. Ho · S. Wang · X. Li (✉)
Institute of Materials Research and Engineering (IMRE), Agency for Science, Technology and Research (A*STAR), 2 Fusionopolis Way, Innovis, #08-03, Singapore 138634, Singapore
e-mail: x-li@imre.a-star.edu.sg

Z. Lin et al. (eds.), *Polymer-Engineered Nanostructures for Advanced Energy Applications*, Engineering Materials and Processes,
DOI 10.1007/978-3-319-57003-7_7

supply for 24 h a day. Since solar power and wind power are intermittent sources, the solution to this problem lies with energy storage. By storing the energy produced at low demand in powerful and reliable batteries/supercapacitors, a constant electricity supply can be provided without reliance on fossil fuels.

Even through the burning of renewable fuel sources such as biomass, energy storage methods are a necessity since variation in electricity production with the variation in demand is not recommended as this decreases the efficiency in production. There have also been numerous studies that have determined that the use of variable generation resources will impact the stability of the grid unless storage is included [1].

Within the realm of energy storage, there are several methods available which all store energy in different forms. Chemical energy storage encompasses many fields including hydrogen storage [2] and methane storage [3]. Another way is the storage of mechanical energy using constructions such as flywheels which are capable of storing 1 kWh of useable energy [4, 5]. Carbon nanotubes (CNTs) are of particular interest in the development of strong materials for flywheels, and as such, CNT-reinforced nanocomposites have been developed [6, 7].

Another type of energy storage is electrochemical energy storage, of which batteries and fuel cells are prime examples. Electrochemical cells are capable of generating electrical energy from chemical reactions as such their voltage is dependent upon the electrode potentials of each of the half-cells in use. For example, rechargeable lithium cells can provide voltage of around 3 V with good cycling capability. Lithium-ion batteries use intercalated lithium compounds as the cathode material, while the anodic material is most commonly graphite, though there is research into alternative electrode materials due to its limited theoretical capacity that is unsuitable for high-energy applications [8–10].

There are many materials that are currently being researched for their potential energy storage applications. One such material would be conductive polymers which are organic polymers that demonstrate as semiconductors most of the time. Conducting polymers store and conduct charge through redox processes; i.e., when oxidation (doping) occurs, ions are transferred to the polymer backbone, and the reverse occurs with reduction (dedoping), wherein ions are released back into solution [11]. The bulk of the film is responsible for charging, and as such, conducting polymers present the opportunity for high levels of specific capacitance. While long-term stability is expected to be a problem due to swelling and shrinking, some research has demonstrated stability over thousands of cycles [12, 13].

A rapidly developing area of research is focussed on electrical energy storage through systems such as superconducting magnetic energy storage which involves storing electrical energy in the form of direct current (DC) electricity that is the source of a DC magnetic field and has been shown to be capable of storing 1–3 MJ of energy with power outputs of up to 2 MW [14]. The conductor operates at cryogenic temperatures where it has relatively no energy losses because the magnetic field is in the superconducting region [14].

The energy storage area in which carbon-based nanofibres have been most prevalent is supercapacitors which are currently used in applications that require

many rapid charge and discharge cycles. Supercapacitors are constructed with two metal foils that act as current collectors, coated with an electrode material such as activated carbon or carbon nanofibres which act as the power connection between the electrode material and the external terminals of the capacitor. These electrode materials must have very high surface areas which may be achieved by various methods such as templating or activation. The methods of storing energy within a supercapacitor fall in two categories: electrical double-layer capacitance (EDLC) and pseudocapacitance which will be discussed later [15, 16].

Carbon nanofiber (CNF) composites include combinations of CNFs with metals, metal oxides, or polymers, which can lead to favourable behaviour during energy storage since CNFs store charges using surface properties, while metal oxides and polymers store charges using the body of the material. Combining the two materials allows for EDLC and pseudocapacitance to be used simultaneously in both Faradaic and non-Faradaic processes to store charges [16, 17]. The performance of CNF/metal oxide/polymer composites is largely determined by the dispersion of the CNFs within the matrix. Therefore, the technique used to achieve uniform dispersion plays a key role in the synthesis of CNF composites. There are two main approaches to achieving the dispersion of CNFs within a metal oxide or polymer matrix, melt mixing, and sonication in low viscosity solutions [6, 18, 19].

Carbon-based materials have attracted a lot of attention due to promising properties in their basic forms, i.e. graphene [20, 21], carbon-based nanofibres [22–26], and hierarchically porous carbon materials [27, 28]. The carbon material that has received the most attention recently is graphene, a one-atom-thick sheet of sp^2-bonded carbon arranged in a hexagonal lattice [29]. Graphene is the thinnest known material in the world and can be considered as the basic starting point for building many other carbon materials [29].

Currently, the main commercially used material for anodes is graphite; however, the theoretical capacity of this is limited to 372 mAh g^{-1} which cannot meet the requirements for high energy capacity [8]. Due to this deficiency, researches into other carbonaceous materials such as carbon nanotubes (CNTs), carbon nanofibres (CNFs), ordered mesoporous carbon, and hierarchically porous carbon have been carried out to show much higher capacity. This chapter focuses on the fabrication of polymer nanofibers and carbon-based nanofibres and the use of such materials for energy storage.

7.2 Fabrication Methods for Carbon-Based Nanofibres

7.2.1 History and Properties of Carbon Nanofibres

The first-recorded publication surrounding carbon-based nanofibres is a patent submitted by Hughes and Chambers on the manufacturing of filaments [30]. However, the true significance of these structures was not fully appreciated until

their structure could be analysed through electron microscopy. The first electron microscopy images of carbon nanofibres were observed by Soviet scientists Radushkevich and Lukyanovich. Published in 1952, they showed multi-wall carbon filaments 50 nm in diameter formed by CO decomposition on an iron substrate [31]. Early research was motivated by the wish to limit their formation. Filamentous carbon or carbon filaments were considered a nuisance as they often grew and accumulated upon metallic catalysts used in petrochemical processing and the conversion of carbon-containing gases.

In 1985, Buckminsterfullerene, $C_{60,}$ was observed by Kroto et al. and earned them the Nobel Prize in 1997 [32]. The discovery was followed by a demonstration by Iijima that carbon nanotubes were formed during arc-discharge synthesis of C_{60} [33, 34]. Two years later, Iijima and Ichihashi and Bethune et al. synthesized single-walled carbon nanotubes (SWCNTs) [33, 35]. It was initially suggested that the carbon nanofibres formed through the catalytic chemical vapour deposition method were comprised of a duplex structure, an inner core of amorphous carbon surrounded by graphitic platelets [36, 37]. More recently, it has been shown that the structural arrangement of CNFs can vary significantly when subjected to different reaction conditions including the chemical nature and structure of the catalyst and the composition of the reactants [38].

As the name suggests, CNFs are nanoscale with respect to their diameters. Their small scale provides a promising basis for research into their properties and any modifications that could result in porosity. While chemical vapour deposition (CVD) was the first process by which CNFs were produced, many processes have since been developed which allow for greater control over structure, morphology, and dopants, while also providing a potentially "greener" approach to production. These methods can include electrospinning [39–41], controlled freezing/freeze-drying [2, 42, 43], and nanofibrous gels and carbonization [22, 44].

7.2.2 Chemical Vapour Deposition

Chemical vapour deposition (CVD) process is often used to produce solid high-quality, high-performance materials. Typically, a substrate is exposed to volatile precursors which may react and/or decompose on or near to a heated substrate surface to produce the desired deposit. Atomistic deposition like this can provide highly pure materials and structural control at atomic or nanometre-scale level [45]. This process can be used to produce single-layer, multi-layer, composite, nanostructured, and functionally graded coating materials [45]. CVD has become one of the main methods for the deposition of thin films and coatings for a wide range of applications including semiconductors for microelectronics, optoelectronics, energy conversion devices, dielectrics for microelectronics, refractory ceramic materials used for hard coatings, protections against corrosion, oxidation or as diffusion barriers, metallic films for microelectronics and for protective coatings, fibre production, and fibre coating [45].

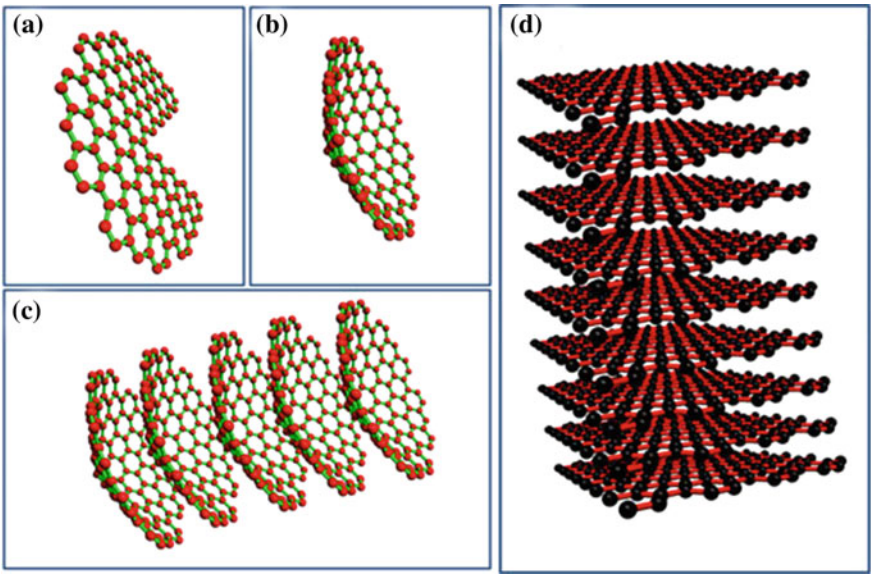

Fig. 7.1 Schematic demonstraction of formation of cup-stacked CNF structure (**a**–**c**), and platelet CNF structure (**d**) (reproduced from Ref. [18] with kind permission of © 2014 Multidisciplinary Digital Publishing Institute)

As mentioned above, CNFs were first presented through a catalytic chemical vapour deposition method involving the iron-catalysed thermal decomposition of carbon monoxide [31]. Small organic molecules such as ethanol can be good precursors for CVD synthesis of CNFs and CNTs since they can decompose to simpler species such as methane, carbon monoxide, and hydrogen. The decomposition of a carbon source on a catalyst causes a solid solution of metal carbides to form, and then, excess carbon atoms in the metal carbide diffuse out from the catalyst to form CNFs. There are often volatile by-products produced through this method; however, these can usually be removed by gas flow through the reaction chamber.

Two types of CNFs can be prepared by CVD, cup-stacked CNFs, and platelet CNFs as shown in Fig. 7.1, [18]. Generally, the structures of CNFs formed are determined by the shapes of the catalytic nanosized metal particles. In a recent study, Lin et al. showed that the participation of chloroform, in a synthesis conducted through the pyrolysis of chloroform and ethanol in the presence of a nickel catalyst, led to Ni–Cl bonding on the surface of the catalyst resulting in a relatively poor crystalline layer and a course surface [46]. Low amounts of chlorine in the catalyst led to the formation of smaller catalyst particles with flat surfaces, causing graphene nanosheets to stack perpendicular to the fibre axis and became platelet graphite nanofibres. A high chlorine content, however, leads to aggregation of the catalyst and thus formation of large catalyst particles with rough surfaces. These rough surfaces resulted in the random stacking of graphene nanosheets which

became turbostratic carbon nanofibres, that is, the sheets of carbon atoms folded or crumpled together haphazardly [46].

7.2.3 *Electrospinning*

As mentioned above, electrospinning is a fibre production method which uses an electric potential to charge polymer solutions or melts and draws them into fibres. The fibres are usually of diameters from tens of nanometers to several microns. Electrospinning shares some characteristics of electrospraying, used in inkjet printing, and conventional dry spinning of fibres [47]. The origins of electrospinning can be dated back to 1934, where Formhals patented an invention relating to the process and producing artificial filaments through the application of 57 kV to a solution of cellulose [48].

When a sufficiently high voltage is applied to a liquid droplet, the body of the liquid becomes charged leading to electrostatic repulsion counteracting surface tension, and therefore, the droplet becomes stretched. At a critical point, a Taylor cone forms, which is the point at which a stream of liquid erupts from the surface of the droplet. A balance between molecular cohesion and conductivity must be achieved so that stream break-up does not occur and a charged jet can be formed [47, 49–52]. The jet dries in flight, and the charge migrates to the surface of the fibre; the mode of current flow changes from ohmic to convective.

Electrospinning is a highly versatile technique that has many variables that can be altered to change the structure of the fibres formed. The morphology of the structures is highly dependent on a combined effect of the electrostatic field and the material properties of the polymer. The charge transport due to the applied voltage is mainly because the polymer jet towards the collector and the variation in current are linked to the mass flow of the polymer from the nozzle tip [51]. For a poly (ethylene oxide)/water system, the fibre morphology changed from a defect-free fibre at the initiating voltage of 5.5 kV to a highly beaded structure at a voltage of 9.0, which was linked to a steep increase in the spinning current which controls bead formation in the electrospinning process [53].

The conductivity of the solution being electrospun is highly important. If the solution is completely insulating or the applied voltage is not high enough for the electrostatic force to overcome surface tension, no fibre can be produced [51]. The solution can be adjusted by adding salt to enhance the conductivity as demonstrated by Qin et al. [54] during their application of different salts to polyacrylonitrile (PAN) polymer solutions. Viscosity and shearing strength of electrospinning solutions are slightly affected by the addition of salts as well as the diameter of the nanofibres produced upon electrospinning, with a correlation being established between the size of the nanofibres formed and the size of the salts [54].

The distance between the nozzle and the collector can easily affect the morphology and structure of electrospun fibres due to the dependence on deposition time, evaporation rate, and whipping/instability interval [51]. A study by

Chang et al. [49] demonstrated the possibility for continuous near-field electrospinning in which solid nanofibres with orderly patterns were deposited over large areas. The needle to collector distance was fixed to 500 μm, while the jet initiation voltage was achieved at 1.5 kV [49]. The polymer concentration greatly affected the morphology of the electrospun nanofibres during this process. When poly (ethylene oxide) concentration was too low, there was insufficient viscoelasticity to suppress capillary break-up [49].

Electrospinning is not just limited to the production of purely polymeric fibres, and a benefit of this process is that solutions can be produced using a variety of materials as well as combinations of materials to produce fibres with unique properties. Combined with carbonization, it is possible to produce highly porous fibres through a number of routes that include spinning into a cryogenic liquid [55], mixing with metal oxide particles [56–59], and coaxial spinning [41, 57] where a material that conventionally would not spin may be encased in a polymer solution that can later be removed through carbonization.

Development of functional composite nanofibres by electrospinning has recently become a research area of intense interest for energy and environmental applications [60–62]. Electrospun nanofibres from polymers with high carbon yields (e.g. PAN in most cases, lignin, cellulose) can be converted to carbon nanofibres through subsequent high-temperature thermal treatment. This generally includes stabilization in air (which converts thermoplastic precursor fibres to highly condensed thermosetting fibres by complicated chemical reactions such as dehydrogenation, cyclization, and polymerization) and carbonization under noble gases. Sometimes, activation steps using steam, base, or acid as the activation agents [63], or hetero-atom doping during the heating treatment process [64], are needed to increase the specific surface area or electrical conductivity of the prepared carbon nanofibres. A unique feature of the electrospun carbon fibres for energy application is that they can form free-standing fibrous mats which can be directly employed as electrode materials for energy devices without using substrates or adding binders and conductive agents, thereby increasing the energy density and simplifying the fabrication process.

The most significant advantage of using electrospun carbon fibres for energy storage is the convenience to fabricate hybrid carbon fibre webs via incorporation of active components (e.g. metal precursors or nanoparticles) or electrically conductive materials (i.e. carbon nanotubes, graphene) to the precursor solutions to improve their electrochemical performance. Electrospinning also offers flexibility in controlling the morphology of prepared carbon nanofibres through variation of the electrospinning parameters (i.e. single or double nozzle, voltage, feeding rate, distance), thermal treatment conditions, as well as precursor compositions. Core–shell-structured electrospun carbon fibres can be created using either a coaxial spinneret [65], or a single spinneret based on the Kirkendall effect during the stabilization process [66, 67]. Hollow or highly porous carbon nanofibres [68–70] can be formed through decomposition or extraction of the incorporated pore-forming components, e.g. poly(methyl methacrylate) (PMMA), Pluronic F127

(a triblock copolymer), and mineral oil. It is also possible to obtain fused carbon fibrous mats by adding low-melting-point polymers in the precursor solutions [71].

7.2.4 Controlled Freezing/Freeze-Drying

Compared to dry-processing routes, wet-shaping techniques are capable of producing materials with complex shapes that can satisfy a large range of applications through the fabrication of dense and porous materials [42]. Freeze-drying, also known as lyophilization, is an industrial dehydration process which works by freezing the material and reducing the surrounding pressure to allow any frozen water to sublimate and desorb under vacuum. The voids of ice crystals after sublimation generate porosity in the dried materials. This is how freeze-drying or more accurately ice templating can be used to produce a range of porous materials. The control of the freezing condition is the key to the tuning of pore morphology. For example, a directional freezing procedure may be employed, as illustrated in Fig. 7.2, allowing for the achievement of aligned microchanneled structures in the direction of freezing after removing the frozen solvent [72–75]. Importantly, the emulsion templating and ice templating can be combined to produce materials with systematically tuned porosity and provide an exciting route for the preparation of aqueous, organic, and poorly water-soluble drug nanoparticle suspensions [76–78].

With the ice-templating method, polymer solutions or colloidal suspensions are usually employed to produce a wide range of porous materials. However, when the

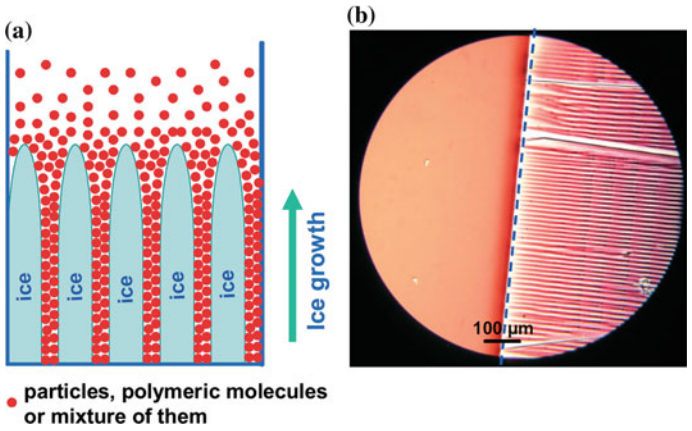

Fig. 7.2 **a** Schematic representation of the directional freezing process. As ice crystals grow in one direction, solutes such as particles and/or polymeric molecules are excluded and packed between the crystals. **b** An optical microscopic image showing the directional freezing of gold nanoparticle suspension. The *blue dashed line* indicates the freezing front, while the *red stripes* are concentrated gold nanoparticles excluded from the freezing front (reproduced from Ref. [74] with kind permission of © 2007 Wiley-VCH) (Color figure online)

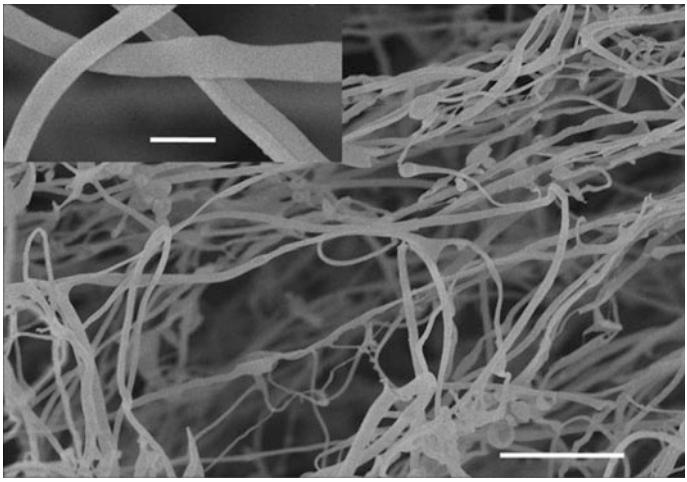

Fig. 7.3 Sodium carboxymethyl cellulose (Mw 250 K) nanofibers prepared by controlled freezing and freeze-drying of its aqueous solution (0.02 wt%). *Scale bar* 5 μm and *inset* scale bar 600 nm (reproduced from Ref. [79] with kind permission of © 2009 Wiley-VCH)

concentrations of the polymers or colloids are very low, nanofibrous structures can be formed. For example, dilute aqueous polymer solutions were directionally frozen and freeze-dried to generate polymer nanofibres, as demonstrated with sodium carboxymethyl cellulose (shown in Fig. 7.3), poly(vinyl alcohol), and sodium alginate [79]. These polymer nanofibres could be further used as templates to prepare hollow titania microtubes and iron oxide nanofibres [79]. It was also possible to produce chitosan in porous and nanofibrous structures for the controlled release of bovine serum albumins [80] or chitosan/silica microsphere composite fibres for dual-controlled release drugs [81]. Dilute colloidal suspensions including metal, metal oxide, and polymers can be subjected to the directional freezing process, which allows the self-assembly of nanoparticles during freezing, and then produce colloids-composed nanofibres after freeze-drying [82–84]. Rather than using polymers or colloids, Mao et al. used the solution of the monomer, 2-hydroxyethyl methacrylate (HEMA), in tert-butyl alcohol. After being directionally frozen and polymerized by ϒ-irradiation, at the temperature the solvent was still frozen, polyHEMA nanofibrous scaffolds were prepared and demonstrated as a highly active and recyclable catalyst support [85].

A general route for production of carbon materials is through the carbonization of polymers. However, to ensure a high carbon yield and maintenance of porous morphology, the polymer should have high carbon content and/or the carbonization procedures may be designed purposely. The controlled freezing-freeze-drying approach has been adopted for lignin solutions [86]. Excitingly, a device was developed to produce a large quantity of lignin nanofibres. The nanofibers were produced in thin films by delivering aqueous lignin solutions through a 0.254-mm aperture onto a liquid nitrogen-cooled drum collector. The resultant frozen ribbons

were then lyophilized to produce a templated lignin network which was then carbonized at 1000 °C to form CNFs [86]. The rapid freezing process described by Spender et al. resulted in elimination of larger lamellar spaces and macropores that had been observed in materials produced through the ice-segregation-induced self-assembly methodology [72, 86, 87].

7.2.5 *Nanofibrous Gels and Carbonization*

Gels are defined as substantially dilute cross-linked systems which exhibit no flow when in the steady state [88]. The skeleton formed in such gels may be maintained by removing the solvent under supercritical condition since pores in the gels are free from capillary forces leaving behind porous, ultralight materials that have extremely low density and thermal conductivity. These aerogels can have high surface areas that could make them ideal as absorbents, catalyst supports, electrodes for electric double-layer capacitors, and materials for chromatographic separation [89].

If a nanofibrous gel can be formed, it is possible to produce a three-dimensional carbon nanofibrous monolith simply by carbonization. The prerequisites for this method are as follows: (1) a dry nanofibrous gel can be formed; (2) there is high carbon content in the gel material; and (3) the nanofibre morphology can be maintained after carbonization. Very often, one can observe the presence of nanofibres in gels, but that may be challenging for the whole gel to be nanofibrous. Perylene diimides are multi-aromatic molecules, with an extended quadrupolar π system, and are utilized in many fields, including biosensing, light-emitting diodes, and pigments. Due to their strong hydrophobicity, self-assembly of perylene diimides can form nanostructures in various organic solvents via π–π interaction/stacking and interaction of side chains.

Liu et al. reported the self-assembly of perylene diimide derivatives by pH-triggered gelation of aqueous solution at room temperature (Fig. 7.4) [22]. After washing with acetone and cyclohexane and then freeze-drying, 3D red porous scaffold consisting of entangled nanofibers with relatively uniform diameters (20–50 nm) was formed as either thin films or monoliths [22]. Upon carbonization, with little shrinkage, the replicated porous scaffolds with carbon nanofibres were successfully prepared (Fig. 7.4). It was very convenient to add different desirable compounds in the solution before gelation. For example, melamine and the surfactant Pluronic P123 could be added to produce *N*-doped mesoporous carbon nanofibres.

In a further development, nanofibrous microspheres were prepared by a water-in-oil emulsion formed with the aqueous perylene diimide derivative solution as the internal phase and *o*-xylene as the external phase [44]. Span 80 was used as the surfactant, and polystyrene (MW 192 K) was added to help stabilize the emulsion. Glucono-d-lactone (GdL) was added into the aqueous phase to initiate the gelation. GdL can be hydrolysed in water and render the solution acidic.

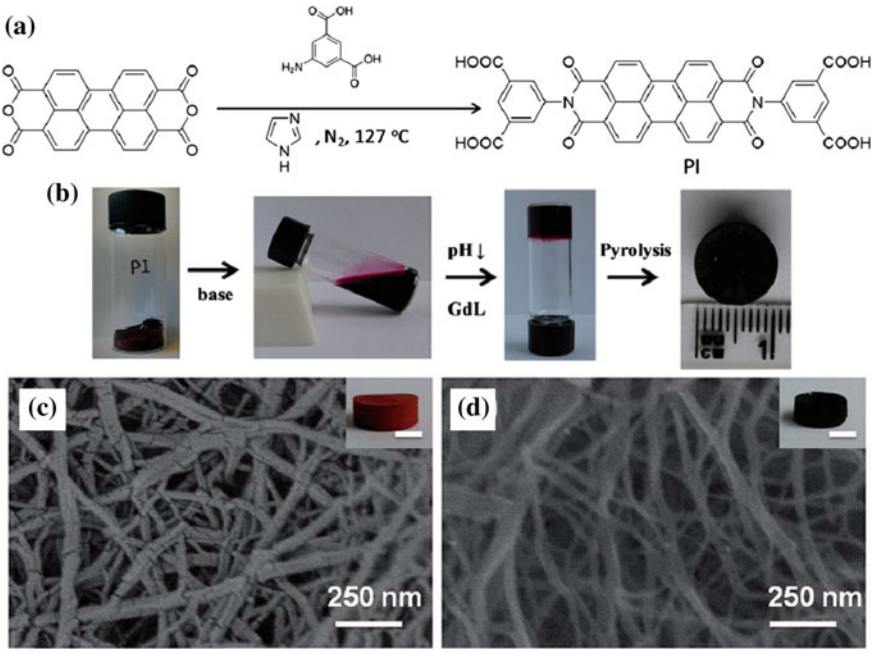

Fig. 7.4 **a** Synthesis and chemical structure of perylene diimide derivative (PI). **b** The procedure of preparing carbon via pH-triggered gelation, freeze-drying, and pyrolysis. **c** The nanofibrous gel structure after freeze-drying (*inset* showing the *red* monolith). **d** The carbon nanofibrous structure after pyrolysis (*inset* showing the *black* carbon monolith) (reproduced from Ref. [22] with kind permission of © 2015 Royal Society of Chemistry) (Color figure online)

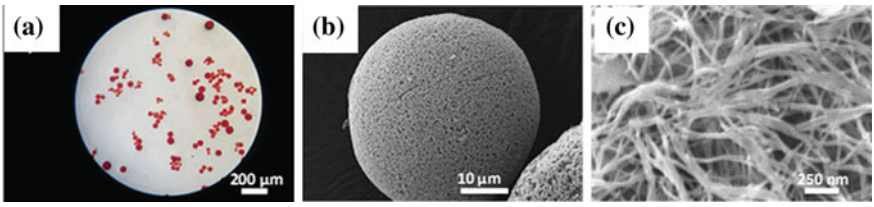

Fig. 7.5 **a** The *red* microspheres by optical microscopy. **b** The porous carbon microsphere. **c** The nanofibrous structure of the carbon microsphere (reproduced from Ref. [44] with kind permission of © 2015 Royal Society of Chemistry) (Color figure online)

The concentration of the GdL was key to producing discreet microspheres; i.e., the lowering pH induced by GdL hydrolysis should not initiate the gelation before a stable emulsion was formed. As shown in Fig. 7.5, porous red microspheres were formed. Upon carbonization, nanofibrous carbon microspheres were produced. This method is unique in that there are not many reports describing the preparation of nanofibrous microspheres. For example, the widely used CVD or electrospinning

would not be able to produce microspheres. Combining this gelation system with a droplet formation method can be a versatile way in preparing nanofibrous microspheres. Apart from the emulsion method, the microfluidic method may be employed to prepare such microspheres.

7.3 Energy Storage Applications

As the population and industrialization of the Earth has increased, so too have the energy demands, putting a great strain on the existing power infrastructure and posing serious implications for the future of a society so dependent on finite energy sources. Up to now, oil-based fuels have been largely used. However, with increasing limitations on the availability of such resources, a need for alternative energy sources has become apparent. New technologies have been developed which rely on sustainable energy forms such as wind energy, solar power, hydroelectricity, and geothermal energy. These methods of energy production provide some measures of the solution needed. However, they are also unpredictable in their generation since it is not always windy and sunny. Due to this inconsistency, renewable sources must be paired with a reliable form of energy storage which can store energy as mentioned above.

It is possible to store energy using several different methods which include chemical (e.g. hydrogen, liquid nitrogen, oxyhydrogen, and vanadium pentoxide), electrochemical (e.g. batteries and fuel cells), electrical (e.g. supercapacitors and superconducting magnetic energy storage), thermal, and mechanical energy. In this section, we will evaluate emerging technologies in the field of energy storage and how carbon-based nanofibres are proving to be useful materials in many applications. Table 7.1 lists the energy storage applications where carbon-based nanofibers have been used.

7.3.1 Rechargeable Batteries

Rechargeable batteries, while initially costing more than the alternative primary batteries that can only be used until completely discharged and then must be disposed, cost much less over the lifetime of ownership in comparison. Their ability to cycle discharging and recharging makes them ideal for use in power stations that must vary their output as demand varies.

7.3.1.1 Li-Ion Batteries

Primary Li batteries were commercialized during the 1970s and involved using lithium metal electrodes. Li–Li_xMnO_2 was one of the systems developed by

Table 7.1 Carbon-based nanofibres for different energy storage systems and their capacities

Type of storage	Material	Capacity	Cycles
Lithium-ion batteries	Nitrogen-doped porous carbon nanofiber webs [90]	Specific: 943 mAh g^{-1} (max)	600
		Reversible: 773 mAh g^{1} (1.0 A g^{-1})	10
	Bubble-nanorod-structured Fe_2O_3- carbon nanofibres [91]	Discharge: 812 mAh g^{-1} (1.0 A g^{-1})	300
Lithium-air batteries	Co_3O_4/carbon nanofibre composite [92]	Initial: 760 mAh g^{-1} (0.5 A g^{-1})	–
	Free-standing thin webs of activated carbon nanofibres [93]	Discharge: 6099 mAh g^{-1} (0.2 A g^{-1}) (Activation Temp: 1273 K)	–
Lithium-sulfur batteries	Coaxial graphene wrapping over sulfur-coated carbon nanofibres [71]	Initial: 745 mAh g^{-1}	–
		Reversible: 273 mAh g^{-1}	1500
	Free-standing carbon nanofibre interlayer—CO_2-activated CNFs [94]	Reversible: 1215 mAh g^{-1}	100
		Reversible: 910 mShg^{-1}	200
Sodium-ion batteries	Polyvinyl chloride nanofibres [95]	Initial: 178 mAh g^{-1} (1.2 A g^{-1})	–
		Reversible: 215 mAh g^{-1} (0.12 A g^{-1})	120
	MoS_2/carbon nanofibre membranes by electrospinning [56]	Charge: 283.9 mAh g^{-1} (0.1 mA g^{-1})	600
		Initial: 381.7 mAh g^{-1} (0.1 A g^{-1})	–
Electric double-layer capacitors	Porous nitrogen and phosphorus co-doped carbon nanofibre networks [96]	Specific: 280 F g^{-1} (1 A g^{-1})	–
		94% capacity retention	10,000
	Self-assembled perylene diimide derivatives [22]	Specific: 192 F g^{-1} (1 A g^{-1})	–
		Reversible: 226 F g^{-1} (4 A g^{-1})	1000
Pseudocapacitors	Carbon nanofibre/MnO_2 nanocables [57]	Specific: 311 F g^{-1}	Scan rate: 2 V s^{-1}
	Carbon nanofibres with encapsulated Co_3O_4 nanoparticles [97]	Specific: 586 F g^{-1} (1 A g^{-1})	–
		Reversible: 424 F g^{-1} (2 A g^{-1})	2000
Hybrid capacitors	Hierarchical porous V_2O_5 nanosheets on carbon nanofibres [98]	Specific: 408 F g^{-1} (1 A g^{-1}) 89.3%	–
		Capacity retention (1.2 A g^{-1})	10,000
	Ni-Al layered double-hydroxide nanosheets/carbon nanotubes [99]	Specific: 115 F g^{-1} (1 A g^{-1})	–
		57% Capacity retention (6 A g^{-1})	2000

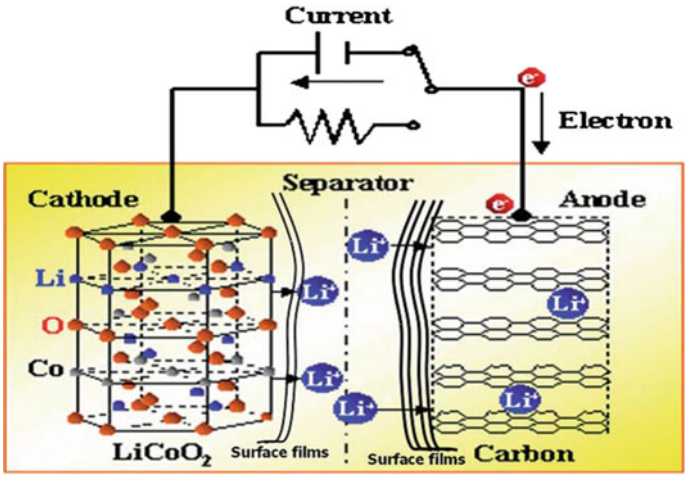

Fig. 7.6 A schematic presentation of the most commonly used Li-ion battery based on graphite anodes and $LiCoO_2$ cathodes (reproduced from Ref. [101] with kind permission of © 2011 Royal Society of Chemistry)

Tadiran, Inc., Israel, for use in mobile phones; however, it did not achieve widespread use due to safety problems [100]. Through further research into lithium as a power source, it became clear that lithium intercalated with transition metal oxides and sulphides could be used as reversible cathode materials for rechargeable Li batteries (Fig. 7.6) [101–103].

Lithium-ion batteries are most commonly found in portable electronic devices which require high cycling durability with a low power to weight ratio. These batteries can supply high energy density while showing small memory effect which can be found in nickel–cadmium batteries as well as some nickel-metal hydride batteries. Memory effect is the loss of charge capacity upon repeated partial charging and discharging. Applying lithium to develop high-performance batteries is motivated by its low standard reduction potential at −3.04 V (vs. the standard hydrogen electrode) as well as its low density, 0.53 g cm^{-3} [104].

During the charging process of Li-ion batteries, lithium ions are forced to leave the cathode material, which is usually lithium-containing metal oxides, under an external electric field and intercalate into a graphite lattice [104]. Bubble-nanorod-structured Fe_2O_3 carbon nanofibres were synthesized by Cho et al. presenting with a discharge capacity of 812 mAh g^{-1} upon its 300th cycle, in comparison with bare Fe_2O_3 nanofibres which showed a discharge capacity of 285 mAh g^{-1} at its 300th cycle with both measurements recorded at current density 1 A g^{-1} [91]. Qie et al. [90] presented porous, nitrogen-doped carbon nanofibre webs as anodes for Li-ion batteries with a higher specific capacity of 943 mAh g^{-1} even after 600 cycles at 2 A g^{-1}. While both processes show high capacities for use in Li-ion batteries, the novelty of the bubble-nanorod-structured Fe_2O_3 carbon

nanofibres presents the possibility of designing greater variations in the material that may present even more promising results.

7.3.1.2 Li-Air Batteries

Li-air batteries have not received much attention until recently due to the particular interest in its potential applications in transportation, where specific energy (energy per unit mass) and energy density (energy per unit volume) are most important [105]. In order to achieve efficiency and range equal to that provided by liquid fuels, a battery system with much higher specific energy and energy density is required. A Li-air battery has notably higher theoretical energy density because the anode metal possesses a high ratio of valence electrons to atomic nuclei and cathode oxygen is not stored in the cell [106]. This theoretical energy density is several times higher than that of state-of-the-art Li-ion battery technology and can even match that of 1700 Wh/kg provided by gasoline energy systems [107].

There are many possible reactions involving lithium and air. Depending on the chemical environment and mode of operation, several products may result from the reaction of Li and O_2 as shown in Scheme 7.1, [108]. There are four major types of Li-air battery systems: aqueous, aprotic/non-aqueous, all-solid-state, and hybrid. Each of these systems is classified by the type of electrolyte used. In particular, the non-aqueous system has attracted a lot of attention due to its potentially high energy density and rechargeability [107].

There is much research necessary for the development of practical Li-air batteries and commercialization. These include quantitatively demonstrating chemical reversibility of the electrochemical reactions (and their relationship to the discharge/charge currents) and understanding coulombic efficiency of the battery in cycling. Furthermore, the investigation of various functional materials has been highly active, covering oxidation-resistant electrodes and cost-effective catalysts (to reduce overpotentials for charge/discharge reactions where insoluble products are formed), new nanostructured air cathodes for optimal transport to active catalyst surfaces, and robust Li metal or composite electrode (capable of repeated cycling at high current densities). Also of great importance is the preparation of high-throughput air-breathing membranes that separate O_2 from ambient air (H_2O and CO_2 limit lifetime of Li-air batteries) and understanding and limiting of the origin of temperature dependences in Li-air batteries [109].

Recent work by Song et al. [92] on Li-air batteries has focussed on composites of Co_3O_4 and carbon nanofibres that were produced through the carbonization of Zeolitic Imidazolate Framework (ZIF)-9/PAN fibrous mats electrospun from dimethylformamide (DMF) solutions. The initial discharge capacity was presented

$$O_2 + 4Li^+ + 4e^- \leftrightarrow 2Li_2O \quad E_{rev} = 2.91\ V$$
$$O_2 + 2Li^+ + 2e^- \leftrightarrow 2Li_2O_2 \quad E_{rev} = 2.96\ V$$

Scheme 7.1 Cell reactions of lithium and oxygen

at 760 mAh g^{-1} at a current density of 0.5 A g^{-1}, which retained 55% of its total capacity after 10 charge/discharge cycles [92]. This may be compared with an initial discharge capacity of CO_2-activated carbon nanofibres of 699 mAh g^{-1} presented by Nie et al. [93] at a current density of 0.2 A g^{-1}; however, it is worth noting that this cathode was not activated until reaching a temperature of 1273 K. The capacity of an electrode is also greatly dependent on the current density being used during measurements. A low current density will usually present with a greater capacity though this may not be suitable for real-life use.

7.3.1.3 Li-S Batteries

While Li-S and Li-air (referred to as Li–O_2 since O_2 is the fuel) share the same anode and have active cathode components (S and O_2) that are neighbours in group 16 of the periodic table, there are important differences regarding their chemistry and the states of their cathodes [110].

Advantages of lithium-sulphur batteries over other rechargeable battery systems include their high specific energy with low costs. Disadvantages, however, include poor electrochemical stability caused by diffusion of polysulphides from the cathode to the anode known as the shuttle effect. Solutions to preventing this migration and confining sulphur within the cathode region include the use of porous carbon structures [104, 111–113], inorganic oxides, and polymers.

Work by Ji et al. [114] pioneered developments of conductive mesoporous carbon frameworks to encapsulate sulphur nanofiller growth within its channels. The mesoporous structure allowed for access of Li^+ for reactivity with the sulphur while also inhibiting diffusion within the framework and the properties of the carbon helped in trapping polysulphides that are formed during redox. Reversible capacities of up to 730 mAh g^{-1} were obtained at C/5 rate after 150 cycles of charge/discharge after modifying the surface of hollow carbon nanofibres (as shown in Fig. 7.7) to prevent the detachment of Li_xS from the carbon surface and achieve specific capacities close to 1180 mAh g^{-1} with a capacity retention of 80% over 300 cycles [114–116].

7.3.1.4 Na-Ion Batteries

With the increase in portable electronics use, the prices of lithium-ion batteries have increased correspondingly. As more applications adopt lithium-ion batteries as power supplies, the strain on lithium sources is expected to increase to the point of running out and efforts to find new sources of the metal and recycle existing batteries will likely lag behind the current demands. An alternative to lithium lies in the development of sodium-ion batteries since it is possible for Na-ion batteries to be comparable if a cathode with 200 mAh g^{-1} capacity and a 500 mAh g^{-1} capacity anode can be discovered. Sodium is also the 4th most abundant element in the crust of the Earth making supply a much smaller issue [117].

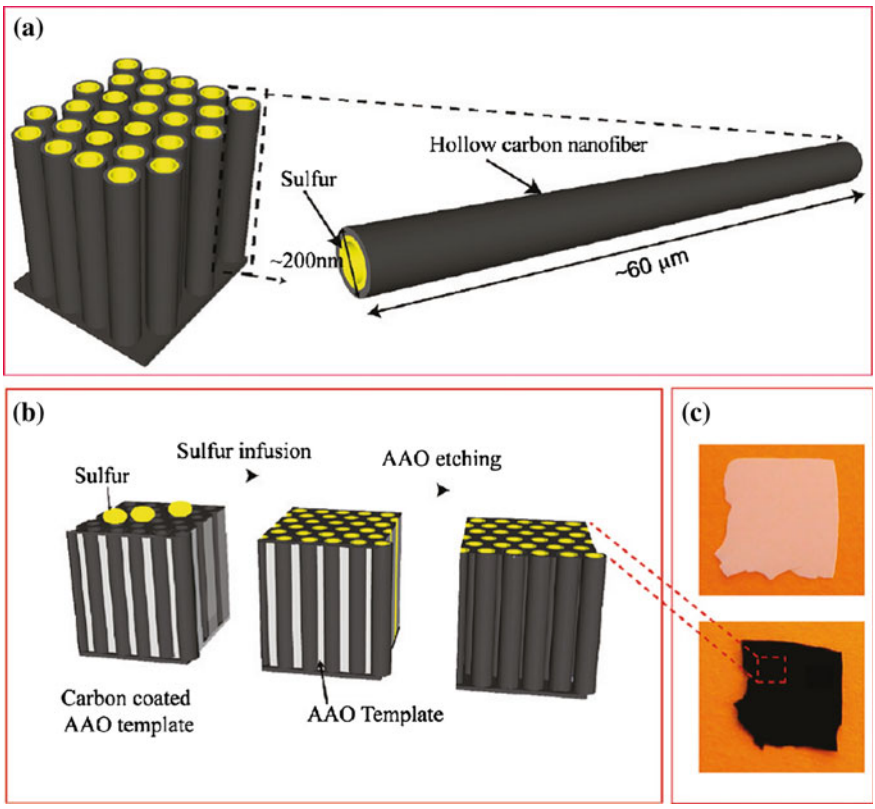

Fig. 7.7 Schematic design and fabrication process of hollow carbon nanofibres/sulfur composite structure. **a** Design principle showing the high aspect ratio of the CNF for effective trapping of polysulphides and **b** the fabrication process of carbon/sulfur cathode. **c** Digital camera images showing the contrast of AAO template before and after carbon coating and sulfur infusion (reproduced from Ref. [116] with kind permission of © 2011 American Chemical Society)

While sodium-ion devices are still in the early stages of development, they are promising for large-scale grid applications in spite of the high cost involved in production of sodium-containing precursors used to make components. To evaluate the potential of sodium-ion batteries as a replacement for lithium-ion, Ong et al. [118] provided a comparison between the two using similar materials operating in Li-ion and Na-ion systems. The larger mass and ionic radius of sodium to lithium as well as various thermodynamic parameters affect a ~300 mV higher standard reduction potential of sodium.

Doping nitrogen into the carbon-based anodes generated extrinsic defects which enhance reactivity and electronic conductivity. The sites at which nitrogen has been added can also adsorb lithium ions and improve lithium storage [90, 119]. This knowledge was used by Wang et al. [120] to improve the capacity of sodium-ion batteries using functionalized, interconnected carbon nanofibres doped with

nitrogen. The N-doped sites and functionalized groups were suggested as the cause for a high current density of 134 mAh g^{-1} after 200 cycles at 0.2 A g^{-1} due to their ability to capture sodium ions rapidly and reversible through surface adsorption and surface redox reactions [120].

Carbon materials with a large interlayer distance and disordered structure are of particular interest to the area surrounding sodium-ion batteries since these properties make them beneficial for Na^+ insertion/extraction [117]. In a study by Bai et al., polyvinyl chloride nanofibres were prepared though electrospinning and pyrolysis at increasing temperatures (600–800 °C) and used as anodic materials in a Na-ion cell, giving an initial reversible capacity of 271 mAh g^{-1} and retain 215 mAh g^{-1} after 120 cycles at 0.012 A g^{-1} [95]. While the current density affects the apparent capacity of the electrode material, further tests showed a reversible capacity of 147 mAh g^{-1} at 0.24 A g^{-1} [95].

7.3.2 Supercapacitors

A conventional capacitor stores energy in the form of electrical charge. Two conducting materials are separated by a dielectric. When an electric potential is applied across the conductors, electrons flow and charge accumulates on each conducting plate, which remain charged after the potential is removed until they are brought into contact again. The capacitance is a measure of the energy storage capability and is related to the amount of charge that can be stored at an applied potential.

The early patent surrounding electrochemical capacitors dates back to 1957 where a capacitor based on carbon with a high surface area was described [121]. Supercapacitors consist of two electrodes with extremely high surface areas kept separate by an ion-permeable membrane that is used as an insulator to protect the electrodes against short-circuiting. A liquid or viscous electrolyte that can be either organic or aqueous is added to the cell and enters the pores of the electrodes and serves as the conductive connection between electrodes across the insulator. These cells must be sealed to ensure stable behaviour over its lifetime [13, 122].

Supercapacitor is a colloquial name for capacitors which store energy within an electrochemical double layer at the electrode/electrolyte interface. Electrochemical double-layer capacitor (EDLC) is the name that best describes the storage principle; however, in general, there are contributions to the capacitance other than the double-layer effects. In addition to the capacitance that arises from the separation of charge in the double layer, reactions that occur on the surface of the electrode provide a contribution. The charge that is required to facilitate these reactions is dependent on the potential resulting in a Faradaic "pseudocapacitance" [13].

There are three types of supercapacitors: electrochemical double-layer capacitors, pseudocapacitors, and hybrid types formed by combining both EDLCs and pseudocapacitors.

7.3.2.1 Electric Double-Layer Capacitors (EDCLs)

Previously, all electrochemical capacitors were called double-layer capacitors; however, it became known that double-layer capacitors and pseudocapacitors were part of a new family of electrochemical capacitors. Double-layer capacitance is the electrostatic storage of electrical energy achieved through separation of charge in a Helmholtz double layer at the interface between the surface of a conductor electrode and an electrolytic solution electrolyte. The separation of charge in a double layer is a few angstroms (0.3–0.38 nm) and is static in origin [13]. Double-layer charge storage is a surface process, and as such, the surface characteristics of the electrode greatly influence the capacitance of the cell. Similarly, the connection between the electrode and the rest of the surface should be without the addition of other conductive or binding agents to reduce the mass of electrochemically inactive components present and sustaining a high specific capacitance with sufficiently high conductivity [123].

There are various models that have been developed over the years to explain the electrical processes that take place at the boundary between a solid conductor and an electrolyte. EDLCs have demonstrated good cycling stability as well as rate capability. However, they generally demonstrate low specific capacitance as well as low energy density [16, 17]. An electric double-layer capacitor is most simply made up of two electrodes immersed in an electrolyte yet kept separate by an ion-conduction but electron-insulating membrane [124]. Activated carbon with a large surface area provides a good platform material for double-layer formation since they allow the capture and release of the electrolyte with relatively decreased resistance, though this is dependent on the pore size and the solvated ion size of the electrolyte [125–127].

Work by Xu et al. [96] has shown the production of polyaniline nanofibre networks with a large specific capacitance of 280 F g^{-1} at a current density of 1 A g^{-1}. The polyaniline networks were co-doped with nitrogen and phosphorus since nitrogen doping can cause a shift of the Fermi level which facilitates electron transfer, while phosphorus doping can restrain the formation of unstable surface groups and also widen the potential window to increase the energy density of EDLCs [28, 96, 128–130]. Lu et al. demonstrate a method of producing porous nanofibres that exhibit a relatively high specific capacitance and may be easily scaled up to produce bulk amounts of material, since a drawback of the electrospinning process is a low production rate coupled with safety concerns and costs [123].

Nanofibrous gels formed using perylene diimide derivatives provided good electrode materials after freeze-drying and carbonization. Due to the formation of nanofibres during the self-assembly process, it is facile to incorporate other molecules into the CNFs. In the case of potassium stannate being used as a base to dissolve the perylene derivative, the preparation of Sn-incorporated CNFs was described [22]. This method yielded gels with higher capacities for those formed upon the incorporation of melamine into the gel, 115 F g^{-1} at a scan rate of 1 mVs^{-1}. When F-127 (a water-soluble triblock copolymer) was used as a

sacrificial template for CNFs during the carbonization process, higher surface area and more interconnected micropores/mesopores were achieved. This was believed to contribute positively towards an increased capacitance, 226 F g^{-1} at 4 A g^{-1} over 1000 cycles, through the improved movement of ions [22]. Nanofibrous microspheres produced by Liu et al., mentioned previously, also demonstrated good specific capacitance of 284 F g^{-1} at 1 A g^{-1}, with a 67% capacitance retention after 1000 cycles at a current density of 4 A g^{-1} [44].

7.3.2.2 Pseudocapacitors

Pseudocapacitance is named as such to differentiate it from electrostatic capacitance as it arises from reversible Faradaic reactions occurring at the electrode. The term "pseudo" arises in order to be able to differentiate it from electrostatic capacitance, since the charge transfer that occurs is voltage dependent and so a capacitive phenomenon occurs. There are two types of mechanisms that can cause such a phenomenon: redox reactions and the deposition of ions to form a monolayer.

Redox reactions occur at electrodes made from metal oxides or conducting polymers. In the case of ruthenium oxide, charging and discharging curves arise as a result of overlapping redox reactions as well as a significant double-layer capacitance due to the porous structure of the hydrous oxide [131]. Deposition of ions to form a monolayer on the electrode surface results in a Faradaic charge transfer. If the sites are occupied randomly in a fixed lattice, the Langmuir adsorption equation may be used to determine another equation, as shown in Scheme 7.2, which can be used to describe a pseudocapacitive relationship [132].

While "pure" CNF materials act as EDLCs, the intercalation of metal oxide nanoparticles results in pseudocapacitive action from the nanoparticles with the CNF acting as a conducting support. This makes CNFs particularly favourable as supports, since they can be easily intercalated with nanoparticles in layered structures which improve electronic conductivity while preventing active particles from detaching from the CNF [97]. Aboulali et al. demonstrated encapsulation of Co_3O_4 within electrospun carbon nanofibres producing materials that gave a capacitance of 586 F g^{-1} at a current density of 1 A g^{-1} and presented good cycling stability of 74% retention after 2000 cycles at 2 A g^{-1} [97]. The Co_3O_4 nanoparticles were securely dispersed within the CNF matrix, allowing for the pseudocapacitive action

$$C_\phi = \frac{q_1 F}{RT} \frac{Kc \pm \exp\left(\frac{-VF}{RT}\right)}{\left(1 + Kc \pm \exp\left(\frac{-VF}{RT}\right)\right)^2}$$

Scheme 7.2 Equation describing the pseudocapacitive relation caused by the adsorption/desorption of ions on the electrode surface where q_1 is the amount of charge required to form or disperse a complete monolayer, K is the electrochemical equilibrium constant, and V is the electrode potential [13, 131]

of the nanoparticles to occur without being hindered by separation and helped by the conductivity of the CNF matrix [97]. A similar principle was demonstrated by Wu et al. in their encapsulation of iron carbide nanoparticles within iron- and nitrogen-doped carbon nanofibres for use in electrocatalysis [133].

The pseudocapacitive ability of MnO_2 was shown by Zhi et al. when used as a coating for CNFs after carbonization of electrospun PAN fibres from DMF, giving an enhanced specific capacitance of 311 F g^{-1} for the whole electrode and showing remarkable stability in comparison with previously reported CNF/metal oxide coaxial electrodes [57, 134]. A drawback of this process would be the limited scalability of production due to the use of electrospinning which suffers from a low production rate.

7.3.2.3 Hybrid Capacitors (Asymmetric, Composite, Battery Type)

While supercapacitors have attracted an enormous amount of attention due to their various advantages including power density and fast charge/discharge capability, their energy densities are far behind batteries [135]. As such, it is necessary to explore opportunities to increase energy density while maintaining power delivery. Hybrid supercapacitors are typically made up of a carbon electrode from EDLC systems and a battery electrode. If an appropriate combination can be found, an increase in the cell voltage may be obtained, while a battery electrode material will deliver more specific capacitance when compared with activated carbons, thereby improving energy and power density [16].

Figure 7.8 shows the possible approaches to hybrid capacitors. Most hybrid electrochemical capacitors produced have used pseudocapacitive materials as the cathode, because they can accumulate charges through Faradaic processes which can increase the specific capacitance and extend the working voltage [136]. Hybrid capacitors can be assembled using hybrid materials such as mixed different metal oxides or doped conducting polymer materials [136–138].

Wang et al. demonstrated a high-performance asymmetric supercapacitor using carbon-MnO_2 nanofiber electrodes that showed only 6% loss in its initial capacitance after 5000 cycles at 4 A g^{-1} and excellent stability of the cell [135]. This can be compared to research by Li et al. who produced a nickel–aluminium layered double-hydroxide nanosheets/carbon nanotube composite which was then tested for both its electrochemical performance and also its possible application in an asymmetric capacitor [99]. Both electrode materials showed remarkable stability, ability to withstand repeated cycles at reasonable current densities, as well as being able to be easily integrated into a circuit given CNF capabilities to be used without binding agents.

Another example of hybrid capacitor electrode material was recently shown by Li et al. where hierarchical porous V_2O_5 nanosheets on carbon nanofibres were investigated. They demonstrated good electrochemical performance of 408 F g^{-1} at a current density of 1 A g^{-1}, as well as good cycling stability over 10,000 cycles, showing only 10.7% loss in specific capacity [98]. However, an advantage of this

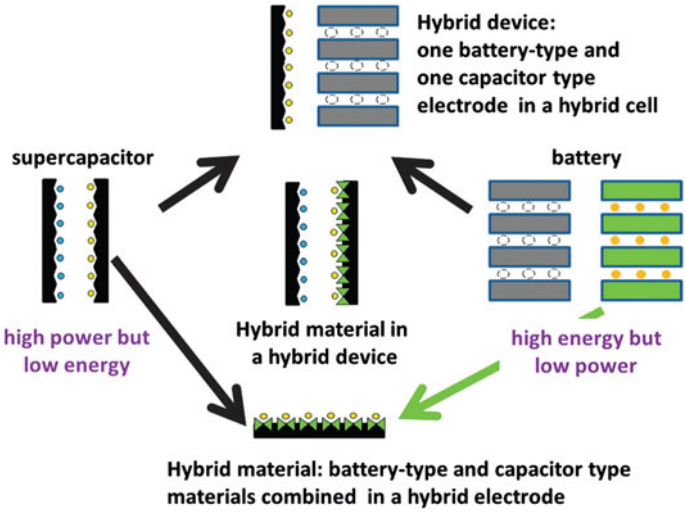

Fig. 7.8 Schematic representation of different hybridization approaches between supercapacitor and battery electrodes and materials (reproduced from Ref. [138] with kind permission of © 2015 Royal Society of Chemistry)

material would be its flexible nature and its ability to retain capacity after bending 200 times showing a robust nature suitable for practical application.

7.4 Conclusion and Outlook

There has been a global increase in demand for energy storage that can provide the high energy density requirements needed for a variety of applications. Carbon nanofibres have been shown to be promising in energy storage. Among the fabrication methods described in this chapter, electrospinning can form free-standing fibrous mats which, after carbonization, can be used without binders, substrates, or conducting agents, thereby increasing the energy density and making fabrication simpler by allowing the fibres to be directly employed as electrode materials. Through variation in feed rate, voltage, solution mix, and distance between the needle and collector, the morphology of fibres may be varied and thus their properties may change. Catalytic chemical vapour deposition is able to produce nanofibres rapidly, and the morphology of the fibres may be altered through the use of different starting materials. However, the instrument with high temperature and high vacuum is required for this technique. Two recently developed methods (controlled freezing and nanofibrous gelation) have been used to prepare polymer nanofibers, which can then be carbonized to produce carbon nanofibers. Polymers with high carbon content may have to be used. It is also more convenient to produce a large quantity of nanofibers with the latter two methods.

These carbon-based nanofibres have shown promising applications within the realm of rechargeable batteries, whether the cell be Li-ion, Li-air, Li-S, or Na-ion. Due to the interlayer spacing in CNFs, it is possible for metal ions to intercalate into a CNF-based anode during the charging process of the cell and be released later while showing relatively good cycling capability. Problems with batteries arise due to shortages of lithium as well as the "shuttle" effect that occurs in Li-S batteries and side reactions that occur in Li-air cells. While sodium is relatively abundant and inexpensive, achieving the appropriate capacity for use in transportation has been a problem, though Na-ion batteries have been shown to be good for use in grid applications. As electrode materials for supercapaitors, the carbon-based nanofibres have demonstrated high capacity and high recyclability. The porous CNFs, when co-doped with nitrogen and phosphorus, demonstrated an increase in energy density and facilitated electron transfer. The incorporation of metal oxides into the CNF matrix leads to an effective pseudocapacitive system due to redox reactions and/or the formation of a monolayer through deposition of ions. The use of CNF electrodes is also reported in hybrid capacitors.

However, to employ the carbon-based nanofibres for the perspective industrial energy storage applications, the materials need to be produced at a large scale with reproducible morphology and physical properties. The preparation conditions are required to be optimized with regard to control of the diameter, porosity, and doping composition of the nanofibers. The optimization of the procedures for preparing the electrodes and assembling the devices (e.g. batteries, supercapacitors) is equally important for safe and efficient use of this technology to meet the increasing energy demand.

Acknowledgements AH is grateful for the University of Liverpool and the A*Star Research Attachment Programme (ARAP) to fund the joint PhD studentship.

References

1. Denholm P, Ela E, Kirby B et al (2010) The role of energy storage with renewable electricity generation (Technical Report). National Renewable Energy Laboratory, Golden, pp 1–61
2. Adeniran B, Mokaya R (2015) Low temperature synthesized carbon nanotube superstructures with superior CO_2 and hydrogen storage capacity. J Mater Chem A 3(9):5148–5161
3. Cao D, Zhang X, Chen J et al (2003) Optimization of single-walled carbon nanotube arrays for methane storage at room temperature. J Phys Chem B 107(48):13286–13292
4. Ahrens M, Kucera L, Larsonneur R (1996) Performance of a magnetically suspended flywheel energy storage device. IEEE T Contr Syst T 4(5):494–502
5. Bolund B, Bernhoff H, Leijon M (2007) Flywheel energy and power storage systems. Renew Sus Energy Rev 11(2):235–258
6. Cha SI, Kim KT, Arshad SN et al (2005) Extraordinary strengthening effect of carbon nanotubes in metal-matrix nanocomposites processed by molecular-level mixing. Adv Mater 17(11):1377–1381
7. Nayfeh TH (2010) High strength composite materials and related processes. US Patent Application 20100203351 A1

8. Winter M, Besenhard JO, Spahr ME et al (1998) Insertion electrode materials for rechargeable lithium batteries. Adv Mater 10(10):725–763
9. Linden D, Reddy TB (2002) Handbook of batteries, 3rd edn. McGraw-Hill, New York
10. Notten P, Bergveld H, Kruijt W (2002) Battery management systems: design by modeling. Kluwer Academic Publisher, Norwell
11. Skotheim TA (ed) (1997) Handbook of conducting polymers. CRC Press, Baco Raton
12. Mastragostino M, Arbizzani C, Soavi F (2001) Polymer-based supercapacitors. J Power Sources 97–98:812–815
13. Namisnyk AM (2003) A survey of electrochemical supercapacitor technology. University of Technology, Sydney
14. Buckles W, Hassenzahl WV (2000) Superconducting magnetic energy storage. IEEE Power Eng Rev 20(5):16–20
15. Zhang LL, Zhao XS (2009) Carbon-based materials as supercapacitor electrodes. Chem Soc Rev 38(9):2520–2531
16. Wang Y, Xia Y (2013) Recent progress in supercapacitors: from materials design to system construction. Adv Mater 25(37):5336–5342
17. Zhi M, Xiang C, Li J et al (2013) Nanostructured carbon-metal oxide composite electrodes for supercapacitors: a review. Nanoscale 5(1):72–88
18. Feng L, Xie N, Zhong J (2014) Carbon nanofibers and their composites: a review of synthesizing, properties and applications. Materials 7(5):3919–3945
19. Shokrieh MM, Esmkhani M, Haghighatkhah AR (2014) Flexural fatigue behaviour of carbon nanofiber/epoxy nanocomposites. Fatigue Fract Eng M 37(5):553–560
20. Cao J, Wang Y, Zhou Y et al (2013) High voltage asymmetric supercapacitor based on MnO_2 and graphene electrodes. J Electroanal Chem 689:201–206
21. Fan Z, Yan J, Wei T et al (2011) Asymmetric Supercapacitors Based on Graphene/MnO_2 and activated carbon nanofiber electrodes with high power and energy density. Adv Funct Mater 21(12):2366–2375
22. Liu X, Roberts A, Ahmed A et al (2015) Carbon nanofibers by pyrolysis of self-assembled perylene diimide derivative gels as supercapacitor electrode materials. J Mater Chem A 3(30):15513–15522
23. Śliwak A, Gryglewicz G (2014) High-voltage asymmetric supercapacitors based on carbon and manganese oxide/oxidized carbon nanofiber composite electrodes. Energy Technol 2(9–10):819–824
24. De Jong KP, Geus JW (2000) Carbon nanofibers: catalytic synthesis and applications. Catal Rev 42(4):481–510
25. Zhang L, Aboagye A, Kelkar A et al (2013) A review: carbon nanofibers from electrospun polyacrylonitrile and their applications. J Mater Sci 49(2):463–480
26. Li W, Zhang F, Dou Y et al (2011) A self-template strategy for the synthesis of mesoporous carbon nanofibers as advanced supercapacitor electrodes. Adv Energy Mater 1(3):382–386
27. Roberts AD, Wang S, Li X et al (2014) Hierarchical porous nitrogen-rich carbon monoliths via ice-templating: high capacity and high-rate performance as lithium-ion battery anode materials. J Mater Chem A 2(42):17787–17796
28. Xu G, Han J, Ding B et al (2015) Biomass-derived porous carbon materials with sulfur and nitrogen dual-doping for energy storage. Green Chem 17(3):1668–1674
29. Allen MJ, Tung VC, Kaner RB (2010) Honeycomb carbon: a review of graphene. Chem Rev 110(1):132–145
30. Hughes TYC, Chambers CR (1889) Manufacture of Carbon Filaments. US Patent 405480
31. Radushkevich LV, Lukyanovich VM (1952) O Strukture ugleroda, obrazujucegosja pri termiceskom razlozenii okisi ugleroda na zeleznom kontakte. Russ J Phys Chem 26:88–95
32. Kroto HW, Heath JR, O'Brien SC et al (1985) C 60: buckminsterfullerene. Nature 318 (6042):162–163
33. Iijima S, Ichihashi T (1993) Single-shell carbon nanotubes of 1-nm diameter. Nature 363 (6430):603–605
34. Iijima S (1991) Helical microtubules of graphitic carbon. Nature 354(6348):56–58

35. Bethune DS, Johnson RD, Salem JR et al (1993) Atoms in carbon cages: the structure and properties of endohedral fullerenes. Nature 366(6451):123–128
36. Baker RTK, Harris PS, Thomas RB et al (1973) Formation of filamentous carbon from iron, cobalt and chromium catalyzed decomposition of acetylene. J Catal 30(1):86–95
37. Baker RTK, Barber MA, Harris PS et al (1972) Nucleation and growth of carbon deposits from the nickel catalyzed decomposition of acetylene. J Catal 26(1):51–62
38. Melechko AV, Merkulov VI, McKnight TE et al (2005) Vertically aligned carbon nanofibers and related structures: controlled synthesis and directed assembly. J Appl Phys 97(4):041301
39. Faccini M, Borja G, Boerrigter M et al (2015) Electrospun carbon nanofiber membranes for filtration of nanoparticles from water. J Nanomater 2015:1–9
40. Aravindan V, Sundaramurthy J, Suresh Kumar P et al (2015) Electrospun nanofibers: a prospective electro-active material for constructing high performance Li-ion batteries. Chem Commun 51(12):2225–2234
41. Lee BS, Yang HS, Yu WR (2014) Fabrication of double-tubular carbon nanofibers using quadruple coaxial electrospinning. Nanotechnology 25(46):465602
42. Li WL, Lu K, Walz JY (2012) Freeze casting of porous materials: review of critical factors in microstructure evolution. Int Mater Rev 57(1):37–60
43. Samitsu S, Zhang R, Peng X et al (2013) Flash freezing route to mesoporous polymer nanofibre networks. Nat Commun 4:2653
44. Liu X, Ahmed A, Wang Z et al (2015) Nanofibrous microspheres via emulsion gelation and carbonization. Chem Commun 51(94):16864–16867
45. Choy KL (2003) Chemical vapour deposition of coatings. Prog Mater Sci 48(2):57–170
46. Wan Y, Yang Z, Xiong G et al (2015) Anchoring Fe_3O_4 nanoparticles on three-dimensional carbon nanofibers toward flexible high-performance anodes for lithium-ion batteries. J Power Sources 294:414–419
47. Bhardwaj N, Kundu SC (2010) Electrospinning: a fascinating fiber fabrication technique. Biotechnol Adv 28(3):325–347
48. Formhals A (1934) Process and apparatus for preparing artificial threads. US Patent 1975504A
49. Chang C, Limkrailassiri K, Lin L (2008) Continuous near-field electrospinning for large area deposition of orderly nanofiber patterns. Appl Phys Lett 93(12):123111
50. Li Z, Wang C (2013) Effects of working parameters on electrospinning. One-dimensional nanostructures. Springer, Berlin Heidelberg, pp 15–28
51. Subbiah T, Bhat GS, Tock RW et al (2005) Electrospinning of nanofibers. J Appl Polym Sci 96(2):557–569
52. Shin YM, Hohman MM, Brenner MP et al (2001) Experimental characterization of electrospinning: the electrically forced jet and instabilities. Polymer 42(25):09955–09967
53. Deitzel JM, Kleinmeyer J, Harris D et al (2001) The effect of processing variables on the morphology of electrospun nanofibers and textiles. Polymer 42(1):261–272
54. Qin X-H, Yang E-L, Li N et al (2007) Effect of different salts on electrospinning of polyacrylonitrile (PAN) polymer solution. J Appl Polym Sci 103(6):3865–3870
55. McCann JT, Marquez M, Xia Y (2006) Highly porous fibers by electrospinning into a cryogenic liquid. J Am Chem Soc 128(5):1436–1437
56. Xiong X, Luo W, Hu X et al (2015) Flexible membranes of MoS_2/C nanofibers by electrospinning as binder-free anodes for high-performance sodium-ion batteries. Sci Rep 5:9254
57. Zhi M, Manivannan A, Meng F et al (2012) Highly conductive electrospun carbon nanofiber/MnO_2 coaxial nano-cables for high energy and power density supercapacitors. J Power Sources 208:345–353
58. Liu H, Bai JIE, Wang QI et al (2014) Preparation and characterization of silver nanoparticles/carbon nanofibers via electrospinning with research on their catalytic properties. NANO 09(03):1450041

59. Savva I, Kalogirou AS, Chatzinicolaou A et al (2014) PVP-crosslinked electrospun membranes with embedded Pd and Cu_2O nanoparticles as effective heterogeneous catalytic supports. RSC Adv 4(85):44911–44921
60. Wang S-X, Yap CC, He J et al (2016) Electrospinning: a facile technique for fabricating functional nanofibers for environmental applications. Nanotechnol Rev 5(1):51–73
61. Cavaliere S, Subianto S, Savych I et al (2011) Electrospinning: designed architectures for energy conversion and storage devices. Energy Environ Sci 4(12):4761–4785
62. Mao X, Hatton TA, Rutledge GC (2013) A review of electrospun carbon fibers as electrode materials for energy storage. Curr Org Chem 17(13):1390–1401
63. Kim B-H, Bui N-N, Yang K-S et al (2009) Electrochemical properties of activated polyacrylonitrile/pitch carbon fibers produced using electrospinning. B Kor Chem Soc 30(9): 1967–1972
64. Qiu Y, Yu J, Shi T et al (2011) Nitrogen-doped ultrathin carbon nanofibers derived from electrospinning: large-scale production, unique structure, and application as electrocatalysts for oxygen reduction. J Power Sources 196(23):9862–9867
65. Hwang TH, Lee YM, Kong B-S et al (2012) Electrospun core-shell fibers for robust silicon nanoparticle-based lithium ion battery anodes. Nano Lett 12(2):802–807
66. Kong J, Tan HR, Tan SY et al (2010) A generic approach for preparing core-shell carbon-metal oxide nanofibers: morphological evolution and its mechanism. Chem Commun 46(46):8773–8775
67. Kong J, Liu Z, Yang Z et al (2012) Carbon/SnO_2/carbon core/shell/shell hybrid nanofibers: tailored nanostructure for the anode of lithium ion batteries with high reversibility and rate capacity. Nanoscale 4(2):525–530
68. Park S-H, Kim B-K, Lee W-J (2013) Electrospun activated carbon nanofibers with hollow core/highly mesoporous shell structure as counter electrodes for dye-sensitized solar cells. J Power Sources 239:122–127
69. Yu Y, Gu L, Wang C et al (2009) Encapsulation of Sn@carbon nanoparticles in bamboo-like hollow carbon nanofibers as an anode material in lithium-based batteries. Angew Chem Int Ed 48(35):6485–6489
70. Wang H, Zhang C, Chen Z et al (2015) Large-scale synthesis of ordered mesoporous carbon fiber and its application as cathode material for lithium-sulfur batteries. Carbon 81:782–787
71. Wang S-X, Yang L, Stubbs LP et al (2013) Lignin-derived fused electrospun carbon fibrous mats as high performance anode materials for lithium ion batteries. ACS Appl Mater Interfaces 5(23):12275–12282
72. Gutiérrez MC, Ferrer ML, del Monte F (2008) Ice-templated materials: sophisticated structures exhibiting enhanced functionalities obtained after unidirectional freezing and ice-segregation-induced self-assembly. Chem Mater 20(3):634–648
73. Qian L, Zhang H (2011) Controlled freezing and freeze drying: a versatile route for porous and micro-/nano-structured materials. J Chem Technol Biotechnol 86(2):172–184
74. Zhang H, Cooper AI (2007) Aligned porous structures by directional freezing. Adv Mater 19(11):1529–1533
75. Zhang H, Hussain I, Brust M et al (2005) Aligned two-and three-dimensional structures by directional freezing of polymers and nanoparticles. Nat Mater 4(10):787–793
76. Wais U, Jackson AW, He T et al (2016) Nanoformulation and encapsulation approaches for poorly water-soluble drug nanoparticles. Nanoscale 8(4):1746–1769
77. Qian L, Ahmed A, Foster A et al (2009) Systematic tuning of pore morphologies and pore volumes in macroporous materials by freezing. J Mater Chem 19(29):5212–5219
78. Zhang H, Wang D, Butler R et al (2008) Formation and enhanced biocidal activity of water-dispersable organic nanoparticles. Nat Nanotechnol 3(8):506–511
79. Qian L, Willneff E, Zhang H (2009) A novel route to polymeric sub-micron fibers and their use as templates for inorganic structures. Chem Commun 26:3946–3948
80. Qian L, Zhang H (2010) Green synthesis of chitosan-based nanofibers and their applications. Green Chem 12(7):1207–1214

81. Ahmed A, Hearn J, Abdelmagid W et al (2012) Dual-tuned drug release by nanofibrous scaffolds of chitosan and mesoporous silica microspheres. J Mater Chem 22(48): 25027–25035
82. Zhang H, Lee JY, Ahmed A et al (2008) Freeze-align and heat-fuse: microwires and networks from nanoparticle suspensions. Angew Chem Int Ed 47(24):4573–4576
83. Shi Q, An Z, Tsung CK et al (2007) Ice-templating of core/shell microgel fibers through 'bricks-and-mortar' assembly. Adv Mater 19(24):4539–4543
84. Shi Q, Liang H, Feng D et al (2008) Porous carbon and carbon/metal oxide microfibers with well-controlled pore structure and interface. J Am Chem Soc 130(15):5034–5035
85. Mao Q, Shi S, Wang H (2015) Biomimetic nanowire structured hydrogels as highly active and recyclable catalyst carriers. ACS Sustain Chem Eng 3(9):1915–1924
86. Spender J, Demers AL, Xie X et al (2012) Method for production of polymer and carbon nanofibers from water-soluble polymers. Nano Lett 12(7):3857–3860
87. Sweetman LJ, Moulton SE, Wallace GG (2008) Characterisation of porous freeze dried conducting carbon nanotube-chitosan scaffolds. J Mater Chem 18(44):5417–5422
88. Ferry JD (1980) Viscoelastic properties of polymers, 3rd edn. Wiley, New York
89. Yamamoto T, Nishimura T, Suzuki T et al (2001) Control of mesoporosity of carbon gels prepared by sol-gel polycondensation and freeze drying. J Non-Cryst Solids 288(1–3):46–55
90. Qie L, Chen W-M, Wang Z-H et al (2012) Nitrogen-doped porous carbon nanofiber webs as anodes for lithium ion batteries with a superhigh capacity and rate capability. Adv Mater 24(15):2047–2050
91. Cho JS, Hong YJ, Kang YC (2015) Design and synthesis of bubble-nanorod-structured Fe_2O_3-carbon nanofibers as advanced anode material for Li-Ion batteries. ACS Nano 9(4): 4026–4035
92. Song MJ, Kim IT, Kim YB et al (2015) Self-standing, binder-free electrospun Co_3O_4/carbon nanofiber composites for non-aqueous Li-air batteries. Electrochim Acta 182:289–296
93. Nie H, Xu C, Zhou W et al (2016) Free-standing thin webs of activated carbon nanofibers by electrospinning for rechargeable Li-O_2 batteries. ACS Appl Mater Interfaces 8(3):1937–1942
94. Singhal R, Chung S-H, Manthiram A et al (2015) A free-standing carbon nanofiber interlayer for high-performance lithium-sulfur batteries. J Mater Chem A 3(8):4530–4538
95. Bai Y, Wang Z, Wu C et al (2015) Hard carbon originated from polyvinyl chloride nanofibers as high-performance anode material for Na-ion battery. ACS Appl Mater Interfaces 7(9):5598–5604
96. Xu G, Ding B, Pan J et al (2015) Porous nitrogen and phosphorus co-doped carbon nanofiber networks for high performance electrical double layer capacitors. J Mater Chem A 3(46):23268–23273
97. Abouali S, Akbari Garakani M, Zhang B et al (2015) Electrospun carbon nanofibers with in situ encapsulated Co_3O_4 nanoparticles as electrodes for high-performance supercapacitors. ACS Appl Mater Interfaces 7(24):13503–13511
98. Li L, Peng S, Wu HB et al (2015) A flexible quasi-solid-state asymmetric electrochemical capacitor based on hierarchical porous V_2O_5 nanosheets on carbon nanofibers. Adv Energy Mater 5(17):1500753
99. Li M, Liu F, Cheng JP et al (2015) Enhanced performance of nickel-aluminum layered double hydroxide nanosheets/carbon nanotubes composite for supercapacitor and asymmetric capacitor. J Alloys Comp 635:225–232
100. Dan P, Mengeritski E, Geronov Y et al (1995) Performances and safety behaviour of rechargeable AA-size Li/Li_xMnO_2 cell. J Power Sources 54(1):143–145
101. Etacheri V, Marom R, Elazari R et al (2011) Challenges in the development of advanced Li-ion batteries: a review. Energy Environ Sci 4(9):3243–3262
102. Gabano J-P (1983) Lithium batteries. Academic Press, London
103. Nazri G-A, Pistoia G (2008) Lithium batteries: science and technology. Springer Science & Business Media, Germany

104. Wu Y, Wang J, Jiang K et al (2013) Applications of carbon nanotubes in high performance lithium ion batteries. Front Phys 9(3):351–369
105. Christensen J, Albertus P, Sanchez-Carrera RS et al (2011) A critical review of li/air batteries. J Electrochem Soc 159(2):R1–R30
106. Peng B, Chen J (2009) Functional materials with high-efficiency energy storage and conversion for batteries and fuel cells. Coordin Chem Rev 253(23–24):2805–2813
107. Ma Z, Yuan X, Li L et al (2015) A review of cathode materials and structures for rechargeable lithium-air batteries. Energy Environ Sci 8(8):2144–2198
108. Yuan J, Yu J-S, Sundén B (2015) Review on mechanisms and continuum models of multi-phase transport phenomena in porous structures of non-aqueous Li-Air batteries. J Power Sources 278:352–369
109. Girishkumar G, McCloskey B, Luntz AC et al (2010) Lithium-air battery: promise and challenges. J Phys Chem Lett 1(14):2193–2203
110. Bruce PG, Freunberger SA, Hardwick LJ et al (2012) Li-O_2 and Li-S batteries with high energy storage. Nat Mater 11(1):19–29
111. Ye H, Yin Y-X, Xin S et al (2013) Tuning the porous structure of carbon hosts for loading sulfur toward long lifespan cathode materials for Li-S batteries. J Mater Chem A 1(22): 6602–6608
112. Chung S-H, Manthiram A (2014) Carbonized eggshell membrane as a natural polysulfide reservoir for highly reversible Li-S batteries. Adv Mater 26(9):1360–1365
113. Zhang Z, Wang G, Lai Y et al (2015) Nitrogen-doped porous hollow carbon sphere-decorated separators for advanced lithium-sulfur batteries. J Power Sources 300:157–163
114. Ji X, Lee KT, Nazar LF (2009) A highly ordered nanostructured carbon-sulphur cathode for lithium-sulphur batteries. Nat Mater 8(6):500–506
115. Zheng G, Zhang Q, Cha JJ et al (2013) Amphiphilic surface modification of hollow carbon nanofibers for improved cycle life of lithium sulfur batteries. Nano Lett 13(3):1265–1270
116. Zheng G, Yang Y, Cha JJ et al (2011) Hollow carbon nanofiber-encapsulated sulfur cathodes for high specific capacity rechargeable lithium batteries. Nano Lett 11(10):4462–4467
117. Slater MD, Kim D, Lee E et al (2013) Sodium-ion batteries. Adv Funct Mater 23(8): 947–958
118. Ong SP, Chevrier VL, Hautier G et al (2011) Voltage, stability and diffusion barrier differences between sodium-ion and lithium-ion intercalation materials. Energy Environ Sci 4(9):3680–3688
119. Zhou Z, Gao X, Yan J et al (2004) A first-principles study of lithium absorption in boron- or nitrogen-doped single-walled carbon nanotubes. Carbon 42(12–13):2677–2682
120. Wang Z, Qie L, Yuan L et al (2013) Functionalized N-doped interconnected carbon nanofibers as an anode material for sodium-ion storage with excellent performance. Carbon 55:328–334
121. Becker HI (1957) Low voltage electrolytic capacitor. US Patent 2800616A
122. Vangari Manisha, Pryor Tonya, Jiang L (2013) Supercapacitors: review of materials and fabrication methods. J Energy Eng 139(2):72–79
123. Lu Y, Fu K, Zhang S et al (2015) Centrifugal spinning: a novel approach to fabricate porous carbon fibers as binder-free electrodes for electric double-layer capacitors. J Power Sources 273:502–510
124. Choi N-S, Chen Z, Freunberger SA et al (2012) Challenges facing lithium batteries and electrical double-layer capacitors. Angew Chem Int Ed 51(40):9994–10024
125. Huang C-W, Hsu C-H, Kuo P-L et al (2011) Mesoporous carbon spheres grafted with carbon nanofibers for high-rate electric double layer capacitors. Carbon 49(3):895–903
126. Portet C, Yushin G, Gogotsi Y (2007) Electrochemical performance of carbon onions, nanodiamonds, carbon black and multiwalled nanotubes in electrical double layer capacitors. Carbon 45(13):2511–2518
127. Largeot C, Portet C, Chmiola J et al (2008) Relation between the ion size and pore size for an electric double-layer capacitor. J Am Chem Soc 130(9):2730–2731

128. Veerasamy VS, Yuan J, Amaratunga GAJ et al (1993) Nitrogen doping of highly tetrahedral amorphous carbon. Phys Rev B 48(24):17954–17959
129. Wang C, Zhou Y, Sun L et al (2013) Sustainable synthesis of phosphorus- and nitrogen-co-doped porous carbons with tunable surface properties for supercapacitors. J Power Sources 239:81–88
130. Hulicova-Jurcakova D, Puziy AM, Poddubnaya OI et al (2009) Highly stable performance of supercapacitors from phosphorus-enriched carbons. J Am Chem Soc 131(14):5026–5027
131. Conway BE, Birss V, Wojtowicz J (1997) The role and utilization of pseudocapacitance for energy storage by supercapacitors. J Power Sources 66(1–2):1–14
132. Langmuir I (1918) The adsorption of gases on plane surfaces of glass, mica and platinum. J Am Chem Soc 40(9):1361–1403
133. Wu Z-Y, Xu X-X, Hu B-C et al (2015) Iron carbide nanoparticles encapsulated in mesoporous Fe-N-doped carbon nanofibers for efficient electrocatalysis. Angew Chem Int Ed 54(28):8179–8183
134. Chen W, Rakhi RB, Hu L et al (2011) High-performance nanostructured supercapacitors on a sponge. Nano Lett 11(12):5165–5172
135. Wang J-G, Yang Y, Huang Z-H et al (2013) A high-performance asymmetric supercapacitor based on carbon and carbon-MnO_2 nanofiber electrodes. Carbon 61:190–199
136. Zhang Y, Feng H, Wu X et al (2009) Progress of electrochemical capacitor electrode materials: a review. Int J Hydrogen Energy 34(11):4889–4899
137. Wang H, Yoshio M, Thapa AK et al (2007) From symmetric AC/AC to asymmetric AC/graphite, a progress in electrochemical capacitors. J Power Sources 169(2):375–380
138. Dubal DP, Ayyad O, Ruiz V et al (2015) Hybrid energy storage: the merging of battery and supercapacitor chemistries. Chem Soc Rev 44(7):1777–1790